Paper No.
08490

Water Effects on Adhesion and Wear Resistance of Chromium Oxide Coatings

Xiaolu Pang[a,b], Alex A. Volinsky[b*], Kewei Gao[a]
a)Department of Materials Physics and Chemistry, University of Science and Technology Beijing, Beijing 100083, China
b)Department of Mechanical Engineering, University of South Florida, Tampa FL 33620, USA

Abstract

Nano-scratch and nano-indentation were used to determine hardness, elastic modulus, adhesion, friction and wear resistance of chromium oxide coatings in air and in water. The friction coefficient is higher in water, compared to air, and it increases with the applied normal load, although there are no obvious differences in hardness and elastic modulus in air vs. water. A higher normal load increases the wear volume; while the wear rate decreases with the number of wear cycles due to machining hardening. A reduction in coating adhesion was observed in water when the normal load exceeded a critical value of 1.8 N.

Key words: moisture, adhesion, friction, wear, chromium oxide

Introduction

Chromium oxide coating has high hardness, low friction, high wear and corrosion resistance, and good optical characteristics,[1-4] therefore it is well suited for wear resistance applications. In the last decade, several attempts have been made to obtain high hardness and good wear resistance by controlling the coating deposition parameters.[5-8] Coating wear resistance and adhesion in sliding contacts strongly

* Author to whom correspondence should be addressed:
Department of Mechanical Engineering University of South Florida, Tampa, FL 33620
Phone: (813) 974-5658 Fax: (813) 974-3539   Email: volinsky@eng.usf.edu

depend on the wear mode and the test conditions in terms of the contact area between the rubbing surfaces modified by the environment .[9]

Coatings mechanical, adhesion and wear properties are strongly affected by the service environment. Premature failure can occur for many reasons including coating delamination, cracking and plastic deformation. In addition to this, thin ceramic PVD coatings usually have columnar grain structure with micro cracks, pinholes, transient grain boundaries and often high through-thickness porosity, which all lead to accelerated pitting corrosion and failure at the coating/substrate interface, especially in hostile environments.[10-14] If one wants to prolong coating life and have good wear resistance, it is important to understand the reliability of chromium oxide coatings in different environments. At the same time, it is important to understand material friction and wear properties at the micro and nano-scales.[15-18]

The size and weight of moving parts is rapidly decreasing with MEMS and data storage technologies development. Novel methods are necessary for nanoscale mechanical characterization. The invention of the atomic force microscope (AFM) enabled mechanical properties measurements of material surfaces at the atomic scale.[19] Friction has been studied with AFM, and in recent years the influence of humidity on friction measurements was demonstrated.[16, 18, 20] There are fundamental differences between conventional lager-scale friction measurements and those performed at the micro and nano-scales. Essential for nano-scale friction measurements is that the tip can be considered as a geometrically well-defined single asperity that slides across the material surface without causing wear. This process, called sliding friction or interfacial sliding, was found to be sensitive to external conditions like environmental humidity or the presence of a liquid phase between the sliding bodies.

This paper reports on the effects of moisture on adhesion and friction of chromium oxide coatings at the nanometer scale. Chromium oxide is used in various environments as a corrosion resistance coating; therefore, investigating its mechanical response in different working conditions is necessary for understanding coating reliability. This insight may open its new applications in MEMS, NEMS and auto/aerospace industries.

Experiment

Chromium oxide coatings were deposited on polished steel substrates by unbiased reactive magnetron sputtering from dual 50.5-mm-diameter Cr targets (99.95% pure) in Ar/O_2 plasma (99.99% pure). The target-substrate separation distance was 60 mm. Deposition was performed at a total pressure of 10^{-1} Pa in a mixed Ar and O_2 atmosphere with 350 W RF power. The argon flow rate was 20 sccm, and the oxygen flow rate was 6.5 sccm.

Prior to deposition substrates were cleaned with acetone and ethanol for 10 minutes in order to remove organic contaminants, and then etched for 15 minutes in Ar plasma at a RF power of 100 W. A 500 nm thick chromium interlayer was sputter deposited for 10 minutes, after which oxygen gas was introduced into the sputtering chamber for the chromium oxide reactive sputter deposition. Substrate temperature reached 473K during the 1 hour deposition process, which produced a 5 μm thick coating.

Hysitron Triboindenter^{TM} was used for the nano-hardness and nano-scratch tests. The nano-harness and Young's modulus were obtained using the method described by Oliver and Pharr.[21] A fused quartz sample was used to calibrate the nano-indenter tip area function in the depth range of interest. A linear ramp from zero to the maximum load of 5 mN was used for the indentation with a three-sided 100 nm tip radius pyramidal Berkovich diamond tip. The same nano-indenter set-up was used for nano-scratch testing. During the nano-scratch test, 90 μN normal force was applied to the diamond tip while it was moving across the sample surface. The high load nano-indenter head was used to delaminate the coating and measure its adhesion in air and in water. Delamination blister geometry was characterized with an optical microscope and with a Tencor P-20H long scan profilometer.

Results and discussion

There are many physical properties that affect coatings' wear resistance, e.g., hardness, elastic modulus, and surface roughness. At first the coating mechanical properties in terms of hardness and elastic modulus were investigated. Table 1 shows the hardness and the elastic modulus of the chromium oxide coatings in air and water environments, with little or no difference between them. The elastic strain to failure, which is related to the ratio of hardness to elastic modulus H/E, has been shown to be a more suitable parameter for predicting wear resistance than hardness alone.[22] It has been shown that H^3/E^2 ratio is proportional to the resistance of the coating to plastic deformation, however, in the present study, the hardness and elastic modulus do not change with the water presence, thus the H/E and H^3/E^2 ratios do not change either.

TABLE 1
HARDNESS AND ELASTIC MODULUS OF COATING IN AIR AND WATER

Environment	H, GPa	E, GPa	H/E	H^3/E^2, GPa
In air	13.0	178.4	0.073	0.069
In water	13.4	177.4	0.075	0.076

For nanoindentation adhesion testing the size of the resulting blister, the load-displacement curve, and the shape of the blister cross-section are necessary to calculate the strain energy release rate, or the practical work of adhesion. The critical buckling stress σ_b and the delamination driving stress σ_d for indentation blisters were

calculated using the following equations:

$$\sigma_b = \frac{\mu^2 E}{12(1-v^2)}\left(\frac{h}{b}\right)^2 \tag{1},$$

$$\sigma_d = \sigma_b\left[c_1\left(\frac{\delta}{h}\right)^2 + 1\right] \tag{2}.$$

The μ^2 is 42.67 for indentation-induced blisters pinned in the center, and $c_1 = 0.2473(1+v) + 0.2231(1-v^2)$. Interfacial fracture toughness, $\Gamma(\Psi)$ can be calculated using the following equation: [23]

$$\Gamma(\Psi) = c\left[1 - \left(\frac{\sigma_b}{\sigma_d}\right)^2\right]\frac{(1-v)h\sigma_d^2}{E} \tag{3},$$

where $c = [1 + 0.9021(1-v)]^{-1}$ [24], h is the coating thickness, b is the blister radius, and δ is the blister height (Fig. 1b). Fig. 1a shows the indentation blisters in air and in water. The blister radius in air is about 42 μm and in water it is 90 μm. Based on equation (3), the coatings adhesion is 22 J/m^2 in air, and it is 0.8 J/m^2 in water, however, the water adhesion result is not quite accurate due to massive coating damage with some of the coating spalling off from the substrate. Equation 3 can only be used for the blisters that are much larger than the indent. Blisters with little or no radial cracking were considered for the adhesion energy measurement, since radial cracking is an additional form of energy dissipation.[23] One can get qualitative result using this formula in wet environment. If one were to use the air blister height and apply it for the wet blister, the adhesion value would be 0.8 J/m^2, which is much smaller than 22 J/m^2 in air.

The reduction in adhesion is primarily due to physical and chemical interactions at the crack tip. The crack propagates at or near the film/substrate interface in the direction perpendicular to the tip vertical motion, and the water reaches the crack front by means of capillary effects. Many papers show crack velocity dependence on relative humidity for films and interfaces.[25-26] If the crack travels at constant velocity,

the energy release rate has to vary along the crack front.

   The reduction of adhesion can be seen with larger delamination radii caused by water diffusion along the interface. At the same time crack velocity was reported as a function of applied load in environments with varying relative humidity. This effect is also seen in our experiments. When indentations were performed at low loads in different environments, there were no obvious changes in adhesion (Fig. 2) since the indents were not deep enough, and the water did not reach the interface.
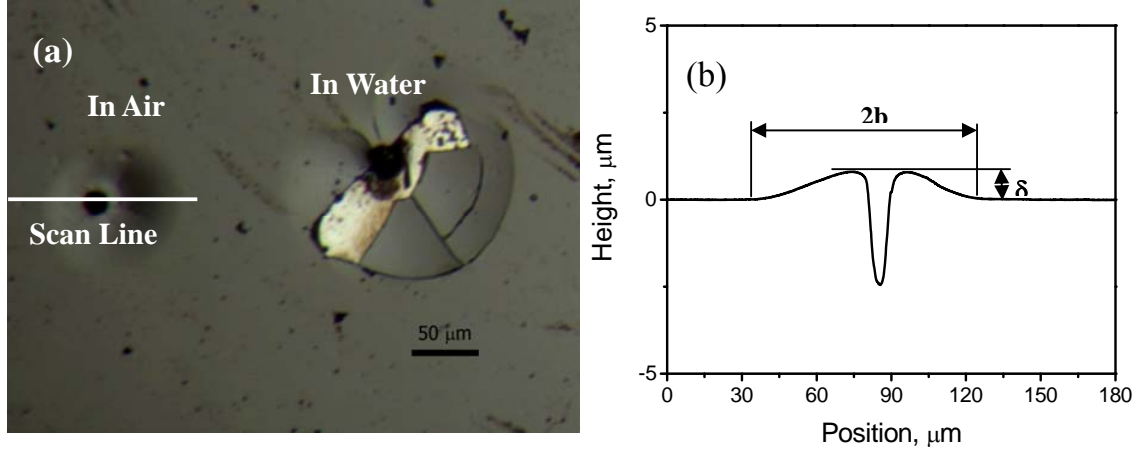

FIGURE 1. a) Indentation Blisters b) Profile Of The Indentation Blister In Air.

   The effect of moisture on interfacial adhesion can be considered by first identifying the rate as which moisture is delivered to the interface, followed by understanding the response of the interfacial adhesion to increased moisture concentration level. Moisture can also cause both reversible and irreversible damage to interfacial adhesion. The loss of interfacial adhesion from moisture is driven by the rate at which moisture is delivered to the interface and the rate of degradation once the moisture reaches the interface. There are three primary mechanisms that contribute to water penetration at the interface. The first mechanism for moisture transport to the interface is diffusion. The second mechanism is attributed to wicking along the interface. The third mechanism for moisture transport to the interface is by capillary action associated with voids and cracks. For our indentation tests, the mechanisms of water reaching the interfaces are the last two. As the indenter tip is driven into the sample forcing film buckling and delamination from the substrate, water is provided a large enough channel to reach the crack tip. Another significant effect of water reaching the interface could be due to lowering the surface energies of the newly formed surfaces at the crack tip.[27] Lower surface energies would result in a lower true work of adhesion:

$$W_A = \gamma_f + \gamma_s - \gamma_{fs} \qquad (4),$$

where γ_f is the film surface energy, γ_s is the surface energy of the substrate and γ_{fs} is the interfacial energy. This could be a reason for larger indentation blisters in water environment.
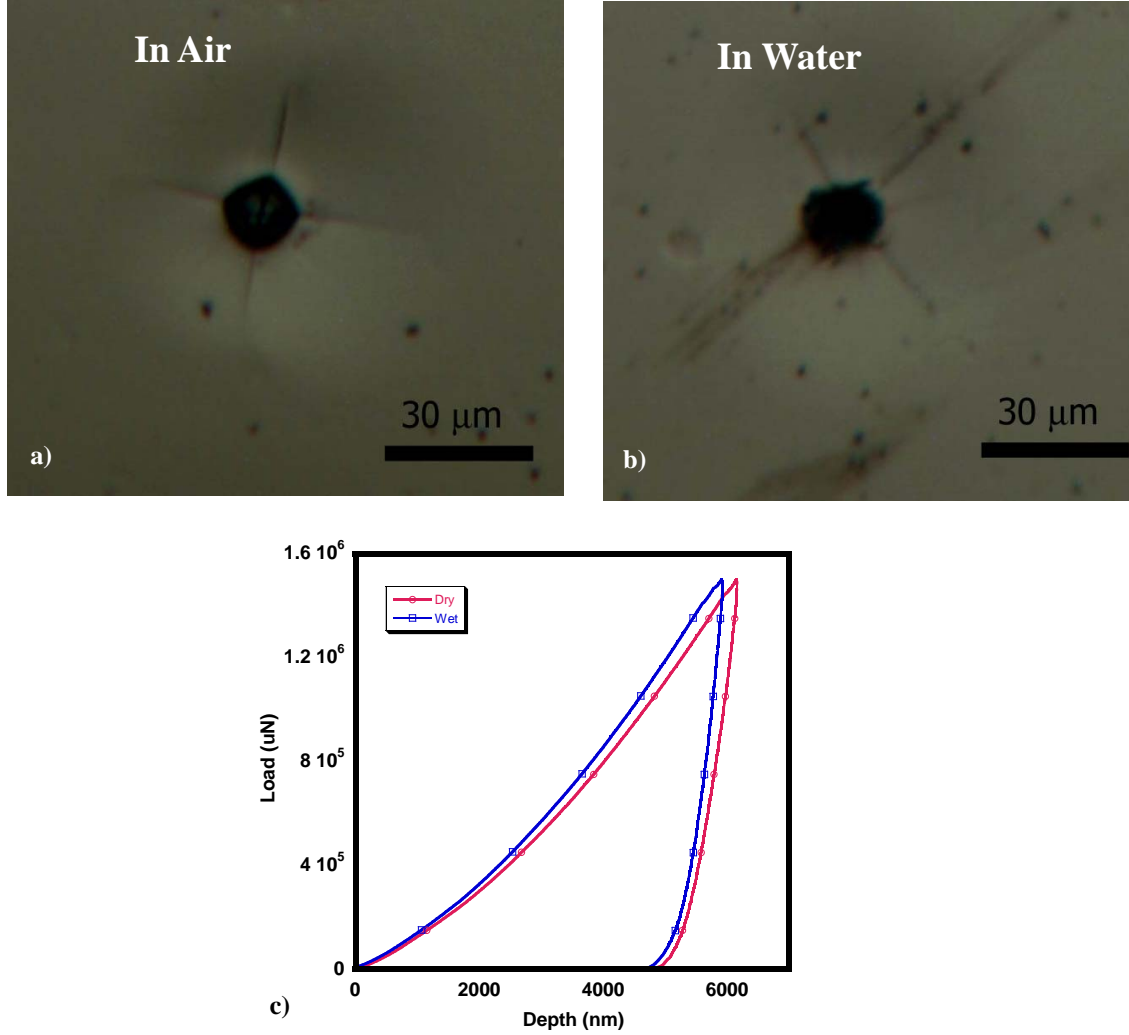

FIGURE 2. Indentation Blisters a) In Air b) In Water at 1.5 N Normal Load, c) Corresponding Load-displacement Curves.

Fig. 3 shows variation of the friction coefficient with the applied normal load in different environments obtained from the scratch test. It is observed that the coefficient of friction on chromium oxide surface increases with the applied normal load in air. It is 0.1 for the 500 μN normal load vs. 0.3 at 3000 μN in air. In this case, the contact area directly affects the adhesive force and increases the friction force, thereby, increasing the coefficient of friction. The average sample surface roughness is about 20 nm, and for the normal load of 500 μN the scratch depth is only 20 to 30 nm. At 3000 μN normal load the scratch depth increases above 100 nm. Therefore, scratching at the lower normal loads just slightly damaged columnar coating grains

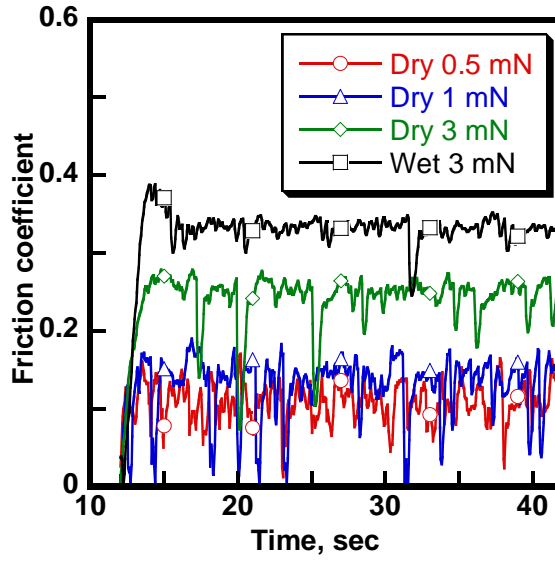whereas the tip penetrated into the coating surface at the higher normal loads.[10]

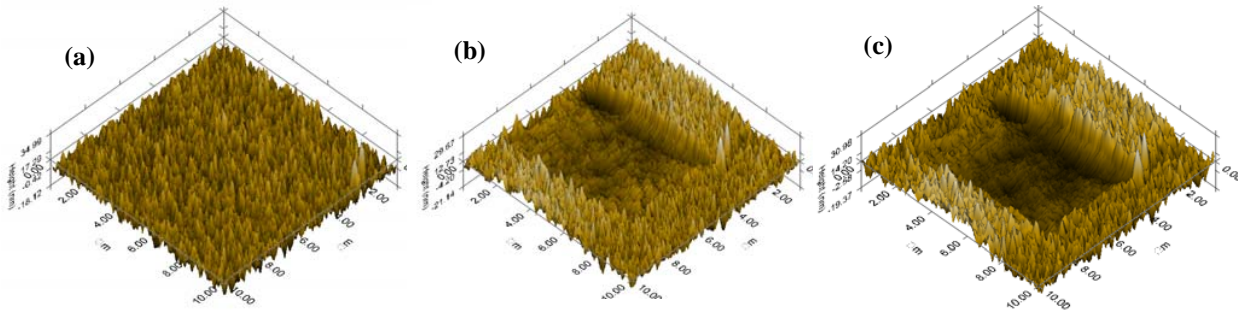FIGURE 3. Friction Coefficients In Different Environments.

FIGURE 4. a) Chromium Oxide Surface Prior To Wear; B) After 500 Cycles Under 90 μN Normal Load, And C) After 900 Cycles Under 90 μN Normal Load.

These results could be explained by considering the fundamental law of friction given by Bowden and Tabor. According to this law, the friction force depends on the real area of contact for a single asperity contact, but the analysis can be extended to multi-asperity contacts as well.[28] Bowden and Tabor assumed that the lateral friction force, F_L, is proportional to the real contact area, A, and to the shear strength, τ.

$$F_L = \tau A \tag{5}.$$

If the shear strength is independent of applied pressure, the friction force is simply proportional to the tip contact area.[28] The friction coefficient is much higher in distilled water than in air, possibly indicating a real increase in contact area and/or added water resistance. At the same time adhesion has also an important role,

especially when measurements are performed in water or other solutions. Many papers report that humidity has a remarkable effect on friction coefficient at the nano-scale.[20, 29-31] Most of them consider variation of the friction coefficient due to changes in the actual contact area and adhesion.
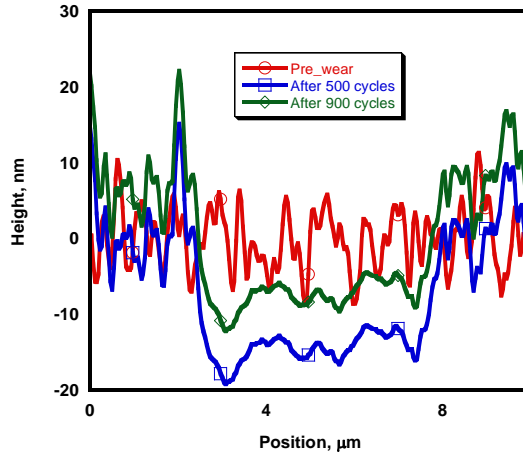

FIGURE 5. Wear Grooves Under 90 µN Normal Load After Different Cycles.

Fig. 4 and Fig. 5 show wear patterns and grooves of chromium oxide coatings after 500 and 900 wear cycles at 90 µN normal load. In contrast, from Fig. 4b and Fig. 4c one can conclude that the wear volume losses increase with increased normal load. Fig. 5 shows that the wear depth is about 16 nm after 500 cycles and 21 nm after 900 cycles. The surface roughness of chromium oxide coatings decreases with increasing wear cycles. The chromium oxide coatings wear rate is different before and after 500 cycles. The wear rate decreases with the number of wearing cycles. There could be several reasons to this phenomenon, and one is depicted by Fig. 6.
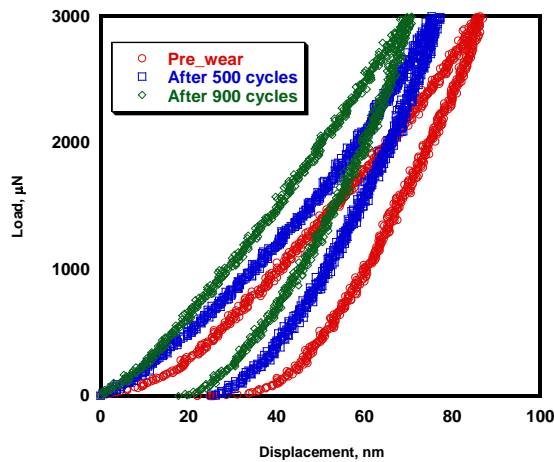

FIGURE 6. Indentation Curves After Different Number Of Wear Cycles In Air.

TABLE 2

HARDNESS AND ELASTIC MODULUS OF CHROMIUM OXIDE COATING AFTER VARYING NUMBER OF WEAR CYCLES

Number of Cycles	Pre-wear	500 cycles	900 cycles
H, GPa	13	14.2	15
E, GPa	178.4	188.4	204.6

Fig.6 shows load-displacement curves of the coating after different number of wear cycles. It was observed that the coating hardness increases with the number of wear cycles (Table 2). The mean values of the coating' hardness and elastic modulus are 13 GPa and 178.4 GPa, respectively, and increase to 14.2 GPa and 188.4 GPa after 500 wear cycles, and to 15 GPa and 204.6 GPa after 900 cycles. There are two main reasons to this phenomenon: one is that the coating stress state was changed after several hundred wear cycles; and the other is that the coating surface density was possibly increased as well.

Conclusions

There is no obvious change in hardness and elastic modulus of chromium oxide coatings in air vs. water environments. The friction coefficient increases with increased normal load in air, at the same time the friction coefficient is much higher in wet than in dry environment under the same normal load. The wear volume increases in air with the increased normal load. The wear rate decreases with the increased number of wear passes due to the machining hardening.

The adhesion of the coating to the substrate is significantly reduced when normal load exceed a critical value of 1.8 N, but there is almost no change in adhesion when the load is lower than this critical value, since water has to reach the interface between the coating and the substrate for the adhesion decrease.[32] If the normal load is smaller than 1.8 N, water molecules can't reach the interface and can't drive the crack propagation and expansion, so there are no effects on the adhesion of coating and substrate.

Acknowledgements

REFERENCES

[1] U. Rothhaar, H. Oechsner: *Thin Solid Films*, 1997, vol. 302, pp. 266-269.

[2] P. Hones, M. Diserens, F. Levy: *Surf. Coat. Technol.*, 1999, vol. 120/121, pp. 277-283.

[3] E. Sourty, J.L. Sullivan, M.D. Bijker: *Trib. Int.*, 2003, vol. 36, pp. 389-396.

[4] F.D. Lai, C.Y. Huang, C.M. Chang, L.A. Wang, W.C. Cheng: *Microelectronic Eng.*, 2003, vol. 67/68, pp. 17-23.

[5] G.V. Samsonov: *The Oxide Handbook*, 2nd edition 1982, 192.

[6] B. Bhushan, G.S.A.M. Theunissen, X. Li: *Thin Solid Films*, 1997, vol. 311, pp. 67-80.

[7] B. Bhushan, B.K. Gupta: *Handbook of Tribology: Materials, Coatings and Surface Treatments,* McGraw-Hill, New York, 1991, Ch. 14

[8] W.J. Lackey, D.P. Stinton, G.A. Cerny, A.C. Schaffhauser, L.L. Fehrenbacker: *Adv. Ceramic Mater.,* 1987, vol. 2, pp. 24-30.

[9] F. Svahn, A. Kassman-Ruddhpi, E. Wallen: *Wear*, 2003, vol. 254, pp. 1092-1098.

[10] X. Pang, K. Gao, H. Yang, L. Qiao, Y. Wang, A. A. Volinsky: *Adv. Eng. Mater.,* 2007, Accepted.

[11] J. Creus, H. Mazille, H. Idrissi: *Surf. Coat. Technol.*, 2000, vol. 130, pp. 224-232.

[12] M. Fenker, M. Balzer, H.A. Jehn, H. Kappl, J.J. Lee, K-H. Lee, H-S. Lee: *Surf. Coat. Technol.*, 2002, vol. 150, pp. 101-106.

[13] E. Andrade, M. Flores, S. Muhl, N.P. Barradas, G. Murillo, E.P. Zavala, M.F. Rocha: *Nucl. Instrum. Methods Phys. Res. B*, 2004, vol. 219/220, pp. 763-768.

[14] C. Liu, A. Leyland, Q. Bi, A. Matthews: *Surf. Coat. Technol.*, 2001, vol. 141, pp. 164-173.

[15] E. Meyer, E. Gnecco: *Nature Mater.*, 2007, vol. 6, pp.180-181.

[16] T. Zykova-Timan, D. Ceresoli, E. Tosatti: *Nature Mater.*, 2007, vol. 6, pp. 230-234.

[17] R. Carpick: *Science*, 2006, vol. 313, pp. 184-185.

[18] A. Socoliuc, E. Gnecco, S. Maier, O. Pfeiffer, A. Baratoff, R. Bennewitz, E. Meyer: *Science,* 2006, vol. 313, pp. 207-210.

[19] G. Binning, C. F. Quate: *Phys. Rev. Lett.*, 1986, vol. 56, pp. 930-933.

[20] M. Binggeli, C. M. Mate: *Appl. Phys, Lett.,* 1994, vol. 65, pp. 415-418.

[21] W. Oliver, G. Pharr: *Journal of Material Research*, 1992, vol. 7(6), pp. 1564-1583.

[22] A. Leyland, A. Matthews: *Wear*, 2000, vol. 246, pp.1-11.

[23] M, Cordill, D, Bahr, N, Moody, W, Gerberich: *IEEE 2004*, vol. 4, pp. 163-167.

[24] J. Hutchinson, Z. Suo: *Adv. Appl. Mech.,* 1992, vol. 29, pp. 64-191.

[25] R. Cook, E. Liniger: *J. Am. Ceram. Soc.*, 1993, vol. 5 pp. 1096-1106.

[26] M. Lane, J. Snodgrass, R. Dauskardt: *Microelectron Reliab.*, 2001, vol. 41, pp. 1615-1624.

[27] A. Volinsky, N. Tymiak, M. Kriese, W. Gerberich:*Mater. Res. Soc. Symp. Proc.*, 1999, vol. 539, pp. 277-290.

[28] E. Gnecco, R. Bennewitz, T. Gyalog, E. Meyer: *J. Phys.: Condens. Matter.*, 2001,

vol. 13, pp. R619-642.

[29] L. Xu, H. Bluhm, M. Salmeron: *Surf. Sci.*, 1998, vol. 407, pp. 251-255.

[30] A. Marti, G. Hahner, N. Spencer: *Langmuir*, 1995, vol.11, pp. 4632-4635.

[31] A. Schumacher, N. Kruse, R. Prins: *J. Vac. Sci. Technol. B*, 1996, vol. 14, pp. 1264-1267.

[32] P. Waters, A. Volinsky: *Exp. Mech.*, 2006, vol. 47, pp. 163-170.